CrossMark

ORIGINAL ARTICLE

Microwave Assisted Synthesis, Physicochemical, Photophysical, Single Crystal X-ray and DFT Studies of Novel Push–Pull Chromophores

**Salman A. Khan[1] · Abdullah M. Asiri[1,2] · Hadi Mussa Basisi[1] ·
Muhammad Nadeem Arshad[1,2] · Kamlesh Sharma[3]**

Abstract Two push-pull chromophores were synthesized by knoevenagel condensation under microwave irradiation. The structure of synthesized chromophores were established by spectroscopic (FT-IR, ^{1}H NMR, ^{13}C NMR, EI-MS) and elemental analysis. Structure of the chromophores was further conformed by X-ray crystallographic. UV-Vis and fluorescence spectroscopy measurements provided that chromophores were good absorbent and fluorescent properties. Fluorescence polarity studies demonstrated that chromophores were sensitive to the polarity of the microenvironment provided by different solvents. Physicochemical parameters, including singlet absorption, extinction coefficient, stokes shift, oscillator strength, dipole moment and fluorescence quantum yield were investigated in order to explore the analytical potential of the synthesized chromophores. In addition, the total energy, frontier molecular orbitals, hardness, electron affinity, ionization energy, electrostatic potential map were also studied computationally by using density functional theoretical method.

✉ Salman A. Khan
sahmad_phd@yahoo.co.in

[1] Chemistry Department, Faculty of Science, King Abdulaziz University, P.O. Box 80203, Jeddah 21589, Saudi Arabia

[2] Center of Excellence for Advanced Materials Research, King Abdulaziz University, P.O. Box 80203, Jeddah, Saudi Arabia

[3] Department of Applied Science, School of Engineering & Technology, ITM University, Sector 23A, Gurgaon 122017, India

Introduction

Nitrogen containing heteroaromatic compounds have attracted a great deal of interest over many years because of their potential applications in different fields e.g. as natural and synthetic bioactive compounds [1], organic reagents [2], DNA intercalators [3], fluorescent dyes [4]. Compound containing with donor (D) and acceptor (A) dienes possessing large second order optical nonlinearities continue to be of interest due to their potential use optical and photonic imaging [5], electrochemical sensing [6], langmuir films and photoinitiated polymerization [7]. The basic design strategy successfully used by many researchers involves the attachment of strong donor (D) and acceptor (A) groups at opposing ends of a л-conjugated bridge [8]. This results in highly polarizable molecules which exhibit large molecular optical nonlinearities [9]. Over the past two decades a number of different л-conjugated bridges have been investigated in order determine the extent to which they impact both the nonlinear optical (NLO) response, as well as other parameters such as thermal stability, photochemical stability and processability/ solubility [10]. Physicochemical characteristics, such as, solvatochromic, piezochromic, oscillator strength, dipole moment, florescent quantum yield and photostability, are also the most important studies for determining the behavior of compounds [11]. Several reactions such as perkin condensation, knoevenagel condensation, aldol condensation were reported for the synthesis of push–pull chromophores. However, knoevenagel condensation is one of the most important reaction for the formation of donor acceptor chromophores by the nucleophilic addition of an active hydrogen compound to a carbonyl group followed by a dehydration reaction [12]. Various synthetic methods have been reported so far, such as refluxing in an organic solvent, the solvent-free solid-phase reaction [13], ultrasonication [14], photosensitization [15] and

🖄 Springer

microwave radiation [16]. 6-methoxy-1,2,3,4-tetrahydro-naphthalin-1-one is good acceptor units and carbazole, pyrrole are the good donor unit in this paper we synthesized push pull chromophore by the reaction 6-methoxy-1,2,3,4-tetrahydro-naphthalin-1-one with carbazole and pyrrole aldehyde by knoevenagel condensation under microwave irradiation and singlet absorption, extinction coefficient, stokes shift, oscillator strength and dipole moment were investigates with single crystal X-ray study. However, the total energy, HOMO, LUMO, hardness (η), electron affinity (EA), ionization energy (IE), electrostatic potential map were also investigated using DFT/RB3LYP method.

Experimental

Chemicals and Reagents

The appropriate aldehyde and 6-methoxy-1,2,3,4-tetrahydro-naphthalin-1-one was purchased from Acros Organic. Other reagents and solvents (A.R.) were obtained commercially and used without further purification, except dimethylformamide (DMF), ethanol and methanol.

Apparatus

Melting points were recorded on a Thomas Hoover capillary melting apparatus without correction. FT-IR spectra were recorded on a Nicolet Magna 520 FT-IR spectrometer. ^{1}H-NMR and ^{13}C-NMR experiments were performed in CDCl$_3$ on a Brucker DPX 600 MHz spectrometer using tetramethyl silane (TMS) as internal standard at room temperature. UV-Vis electronic absorption spectra were acquired on a Shimadzu UV-1650 PC spectrophotometer. Absorption spectra were collected using a 1 cm quartz cell. Steady state fluorescence spectra were measured using Shimadzu RF 5301 PC spectrofluorphotometer with a rectangular quartz cell. Emission spectra were monitored at right angle. All fluorescence spectra were blank subtracted before proceeding in data analyses.

(2E)-2-[(9-Ethyl-9H-Carbazol-3-yl)Methyllidene]-6-Methoxy-3,4-Dihydronaphthalene-1-one(1)

A mixture of 9-ethyl-9H-carbazole-3-carbaldehyde (2 g, 0.0089 mol), and 6-methoxy-1,2,3,4-tetrahydro-naphthalin-1-one (0.0089 mol) in anhydrous ethanol (15 ml), in the presence of few drops of pyridine. Inside the microwave oven the reaction mixture was heated for 2 min. (at 210 watts i.e. 30 % microwave power). When the reaction was completed, reaction mixture was allowed to cool and recrystallized with ethanol and chloroform. Yield: 79.40 %; M.p. 127 °C; EI-MS m/z (rel. Int. %): 383 (78) [M + 1]$^+$; IR (KBr) v_{max} cm^{-1}: 2954 (C-H), 1685 (C = O),1579 (C = C), 1124 (C-N); ^{1}H NMR (600MXz CDCl$_3$) δ: 8.22 (s, 1 H, CH), 8.18 (dd, CH$_{Aromatic}$, J = 3.6 Hz), 8.12 (d, 1 H, CH$_{Aromatic}$, J = 7.8 Hz), 8.08 (s, 1 H, CH$_{Aromatic}$), 8.04 (dd, 1 H, CH$_{Arpmatic}$, J = 1.8 Hz), 7.28 (d, 1 H, CH$_{Aromatic}$, J = 1.2 Hz), 7.58 (, 1 H, CH$_{Aromatic}$, J = 1.2 Hz), 7.42 (s, 1 H, CH$_{Aromatic}$), 6.88(d, 1 H, CH$_{Aromatic}$, J = 2.4 Hz), 6.88 (d, CH$_{Aromatic}$, J = 2.4 Hz), 6.75 (d, 1 H, CH$_{Aromatic}$, J = 2.4 Hz), 6.72 (d, 1 H, CH$_{Aromatic}$, J = 2.4 Hz), 4.45–4.40 (q, CH$_2$-CH$_3$), 3.85 (s, 3 H, OCH$_3$), 2.96–2.91 (m, 2 H, CH$_2$), 2.62–2.60 (m, 2 H, CH$_2$), 1.49–1.44 (t, N-CH$_2$-CH$_3$); ^{13}CNMR (CDCl$_3$) δ: 194.28 (C = O), 186.98, 163.45, 145.55, 140.40, 14.73, 133.10, 130.37, 128.37, 126.84, 123.06, 122.89 120.56, 119.38 (C-Aromatic), 113.20, 109.17, 108.72, 55.47, 38.93, 37.97, 30.19, 29.35, 27.51, 23.40, 13.88, 13.85; Anal. calc.for C$_{26}$H$_{23}$NO$_2$: C, 81.86, H, 6.08, N, 3.67; Found: C, 81.81, H, 6.04 N, 3.62.

6-Methoxy-2-[(1-Methyl-1H-Pyrrol-2-yl)Methylidene]-3,4-Dihydronaphthalen-1(2H)-one (2)

A mixture of 1-methyl-1H-pyrrole-2-carbaldehyde (2 g, 0.018 mol), and 6-methoxy-1,2,3,4-tetrahydro-naphthalin-1-one (0.018 mol) in anhydrous ethanol (15 ml) in the presence of few drops of pyridine. Inside the microwave oven the reaction mixture was heated for 3 min. (at 210 watts i.e. 30 % microwave power). When the reaction was completed, reaction mixture was allowed to cool and recrystallized with ethanol and chloroform. Yield: 88.25 %; M.p. 149 °C; EI-MS m/z (rel. int. %): 269 (72) [M + 1]$^+$; IR (KBr) v_{max} cm^{-1}: 2947 (C-H), 1655 (C = O),1586 (C = C), 1135 (C-N); ^{1}H NMR (600MXz CDCl$_3$) δ: 8.16 (s, 1 H, CH), 8.05 (d, 1 H, CH$_{Aromatic}$, J = 8.4 Hz), 8.08 (d, 1 H, CH$_{Aromatic}$, J = 9.0 Hz), 7.81 (s, 1 H, CH$_{Aromatic}$), 6.82 (d, 1 H, CH$_{Aromatic}$, J = 7.6 Hz), 6.72 (d, 1 H, CH$_{Aromatic}$, J = 3.0 Hz), 6.56 (d, 1 H, CH$_{Aromatic}$, J = 3.6 Hz), 3.68 (s, 3 H, OCH$_3$), 2.95–2.90 (m, 2 H, CH$_2$), 2.64–2.58 (m, 2 H, CH$_2$); ^{13}CNMR (CDCl$_3$) δ: 198.27 (C = O), 187.16, 164.43, 145.97, 145.38, 131.41, 125.97, 122.85, 116.27 (C-Aromatic), 113.76, 109.02, 55.44, 38.93, 36.42, 31.38, 28.63, 27.26; Anal. calc.for C$_{17}$H$_{17}$NO$_2$: C, 76.38, H, 6.41, N, 5.24. Found: C, 76.30, H, 6.35, N, 5.18.

Materials and Method Crystallography

Both the molecule 1 & 2 were crystallized and diffracted under the conditioned provided in Table 1, to understand the geometry of molecules. The crystals were fixed on glass tip supported by magnetic base using glue and mounted on Agilent SuperNova (Dual source) Agilent Technologies Diffractometer, equipped with graphite-monochromatic Cu/Mo Kα radiation for data collection. Initially unit cell were determined before proceeding whole data collection at 296 K under the Cu Kα radiation and data reduction were carried out using CrysAlisPro software

Table 1 Crystal data and structure refinement for chromophore 1 & 2

Identification code	1006471	1006472
Empirical formula	$C_{26}H_{23}NO_2$	$C_{17}H_{17}NO_2$
Formula weight	381.45	267.32
Temperature/K	296.15	296.15
Crystal system	triclinic	orthorhombic
Space group	P-1	Pbca
a/Å	9.0004(4)	14.1214(4)
b/Å	9.1126(4)	7.19510(10)
c/Å	12.5863(6)	27.4963(6)
α/°	87.798(4)	90.00
β/°	89.920(4)	90.00
γ/°	73.257(4)	90.00
Volume/Å^3	987.75(8)	2793.76(11)
Z	2	8
ρ_{calc}mg/mm^3	1.283	1.271
μ/mm^{-1}	0.634	0.664
F(000)	404.0	1136.0
Crystal size/mm^3	0.37 × 0.26 × 0.18	0.42 × 0.16 × 0.14
2θ range for data collection	7.02 to 152.32°	6.42 to 152.84°
Index ranges	−11 ≤ h ≤ 11, −11 ≤ k ≤ 10, −15 ≤ l ≤ 15	−17 ≤ h ≤ 17, −9 ≤ k ≤ 8, −30 ≤ l ≤ 34
Reflections collected	10970	17962
Independent reflections	4116[R(int) = 0.0190]	2911[R(int) = 0.0319]
Data/restraints/parameters	4116/0/264	2911/0/184
Goodness-of-fit on F^2	1.062	1.051
Final R indexes [I > = 2σ (I)]	$R_1 = 0.0401$, w$R_2 = 0.1096$	$R_1 = 0.0383$, w$R_2 = 0.0981$
Final R indexes [all data]	$R_1 = 0.0468$, w$R_2 = 0.1157$	$R_1 = 0.0477$, w$R_2 = 0.1074$
Largest diff. peak/hole/e Å^{-3}	0.20/−0.15	0.17/−0.17

[17]. The structure solution and refinement was performed using SHELXS–97 [18], in-built with X-Seed [19]. All non–hydrogen atoms were refined anisotropically by full–matrix least squares methods [20]. The reflection (0 1 0) was omitted in the final refinement of molecule 1.
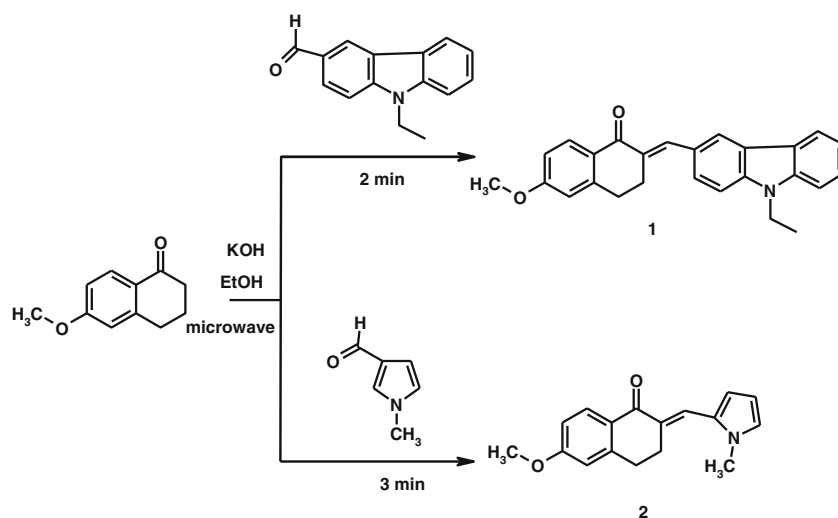
Computational Method

Compound **1** and **2** were optimized using Spartan'08 Windows graphical software [21] by employing Density Functional Theory (DFT) with RB3LYP method. This method has been used successfully for the calculation of small neutral molecules [22]. However, compound **1** and **2** were modeled and optimized using Semiempirical PM3 method followed by the Hartree-Fock method with 6-31G* basis set. The resulting wavefunction, Hessian matrix and geometry were subjected for the final calculation that is DFT with 6-31G* basis set. The asterisk means that the "d" polarization functions were added for C, O and N atoms. The fundamental frequencies of both models were also calculated and assigned as minima (that is all positive frequencies).

Result and Discussion

Chemistry

The synthesis of chromophores are straight forward and the compounds were isolated in good yield (Scheme 1) [23]. The obtained compounds are stable in the solid state as well as in the solution. The structure of the chrompohores were conformed by the spectral data EI-MS, FT-IR, ¹H-NMR, ¹³C-NMR and purity of the chromophores further conformed by the elemental analysis. Assignments of selects characteristic IR band positions provide significant indication for the formation of the chromophores. The chromophore 1 & 2 showed intense bands at 1685 & 1655 cm^{-1} due to ν(C = O) stretch peak of 6-methoxy-1,2,3,4-tetrahydro-naphthalin-1-one. The chromophore 1 & 2 showed intense bands at 1579 & 1586 cm^{-1} due to (C = C) stretch which is confirm the formation of donor accepter chromophore. Further evidence for the formation of chromophores was obtained from the ¹H-NMR spectra, which provide diagnostic tools for the positional elucidation of the protons. Assignments of the signals are based on the chemical shifts and intensity patterns. The

**Scheme 1** Schematic diagram showing the synthesis of choromophore (1 & 2)

aromatic protons of chromophore 1 & 2 are shown as *s,d* and *dd* in the range ppm for the chromophore. A Singlet due to =C-H proton in the chromophore 1 & 2 was observed at δ 8.22 & 8.16 respectively. The appearance of singlet, doublet, and multiplets at δ 6.56-8.18 was due to aromatic protons in chromophore 1 & 2. The appearance of two multiplets at δ 2.96-2.90 and 2.64-2.58 was due to the benzylic protons (C5-*H* and C6-*H* respectively) in chromophore 1 & 2. ^{13}C NMR (CDCl$_3$) spectra of chromophore were recorded in CDCl$_3$ and spectral signals are in good agreement with the probable structures. The carbonyl carbon of the chromophores usually appears at δ 194.28 & 198.27 for chromophore 1 & 2 in ^{13}C NMR spectrum. Details of ^{13}C-NMR spectra of both chromophores are given in the experimental section. Finally characteristic peaks were observed in the mass spectra of chromophore 1 & 2 by the molecular ion peak. The mass spectrum of chromophore 1 & 2 shows a molecular ion peak (M$^{+·}$) m/z 383 and 269. Both chromophore give similar fragmentation pattern.

Single Crystal X-ray of Chromophore 1 & 2

6-Methoxy-3,4-dihydro-2*H*-naphthalen-1-one is present in the both molecules. The root mean square deviation

values for cyclohexenone ring are 0.2375(2) Å & 0.1788(2) Å for chromophores 1 & 2 respectively Figs. 1 and 2. Selected bond lengths and bond angle are given in Tables 2 and 3 respectively. The puckering amplitude parameters are Q = 0.4960 Å, θ = 113.89° & φ = 34.2895° for molecule 1 while Q = 0.4380 Å, θ = 63.63° & φ = 216.4377° for molecule 2. The carbazole moiety in 1 and pyrole in 2 are planer with the r.m.s. deviation of 0.0152(1) Å & 0.0040(1) Å. The dihedral angles between the fused ring systems i.e. aromatic and cyclohexenone, in both molecules are 8.68(7)° and 10.70(4)°. In chromophore 1 carbazole is oriented at dihedral angle of 50.65(4)° with respect to cyclohexenone ring while in chromophore 2 pyrole ring produces the same angle of 39.69(6)°. There is no classical or non-classical hydrogen bonding interaction found in any of structure, neither these posses π-π interaction. The crystal data were deposited at the Cambridge Crystallographic Data Centre and have been assigned the deposition numbers CCDC 1006471 & 1006472 for chromophore 1 & 2. This data can be obtained free of charge from The Cambridge Crystallographic Data Centre via www.ccdc.cam.ac.uk/data_request/cif.

Fig. 1 ORTEP diagram for chromophore 1, drawn at 50 % probability level of thermal ellipsoids
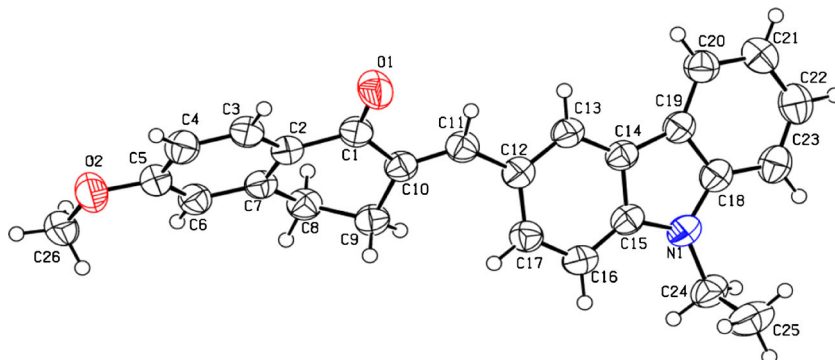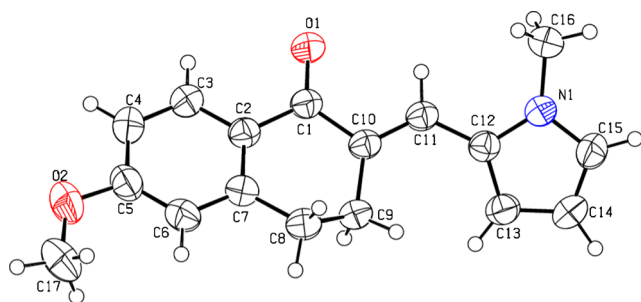
Fig. 2 ORTEP diagram for chromophore 2, drawn at 50 % probability level of thermal ellipsoids

Spectral Behavior of Chromophores (1&2)

The spectroscopic properties of compounds should be solvent dependent owing to their donor-acceptor arrangement. Solvent relaxation usually requires much longer time compared to the time of absorption and fluorescence. Therefore, any solvent stabilization of the ground state or the excited state is usually manifested in clear shift in the spectra of the chromophore. Spectral red shifted in the absorption and the fluorescence are expected in non polar to polar solvents due to the stabilization of the intramolecular charge transfer (ICT) occurring between the donor –acceptor groups. To confirm this hypothesis, the absorption and florescence spectra of chromophores 1 & 2 were investigated in different solvent on the basis of polarities. The absorption properties of the chromophores 1& 2 in different solvents were obtained at room temperature and are shown in Figs. 3a, b and 4a, b, corresponding spectral data are summarized in Tables 4 and 5. An overall red shift of 19 nm and 18 nm are observed in the absorption maxima of chromophores 1 & 2 on going from THF to methanol.

These features indicate a strongly allowed $\pi - \pi^*$ transition with intramolecular charge transfer characters from carbazole and pyrrol group (electron donor group) to keto (electron acceptor group) [24].

Table 2 Selected bond lengths for chromophore 1 & 2

1			2		
Atom	Atom	Length/Å	Atom	Atom	Length/Å
O1	C1	1.2286(15)	O1	C1	1.2337(14)
O2	C5	1.3601(17)	O2	C5	1.3645(17)
O2	C26	1.4218(18)	O2	C17	1.422(2)
N1	C15	1.3784(17)	N1	C12	1.3858(16)
N1	C18	1.3835(18)	N1	C15	1.3561(16)
N1	C24	1.4527(17)	N1	C16	1.4507(18)

Table 3 Selected bond angles for chromophore 1 & 2

1				2			
Atom	Atom	Atom	Angle/°	Atom	Atom	Atom	Angle/°
C5	O2	C26	118.76(12)	C5	O2	C17	118.11(13)
C15	N1	C18	108.91(11)	C12	N1	C16	126.68(11)
C15	N1	C24	125.75(12)	C15	N1	C12	109.30(11)
C18	N1	C24	125.12(12)	C15	N1	C16	124.02(12)
O1	C1	C2	120.41(12)	O1	C1	C2	120.11(11)
N1	C18	C19	109.19(12)	O1	C1	C10	122.00(11)
N1	C18	C23	129.27(13)				

Determination of Oscillator Strength and Transition Dipole Moment

The solvatochromic behavior in chromophores (**1 & 2**) allows one to determine the difference in the dipole moment between the excited singlet and the ground state ($\Delta\mu = \mu_e - \mu_g$). This
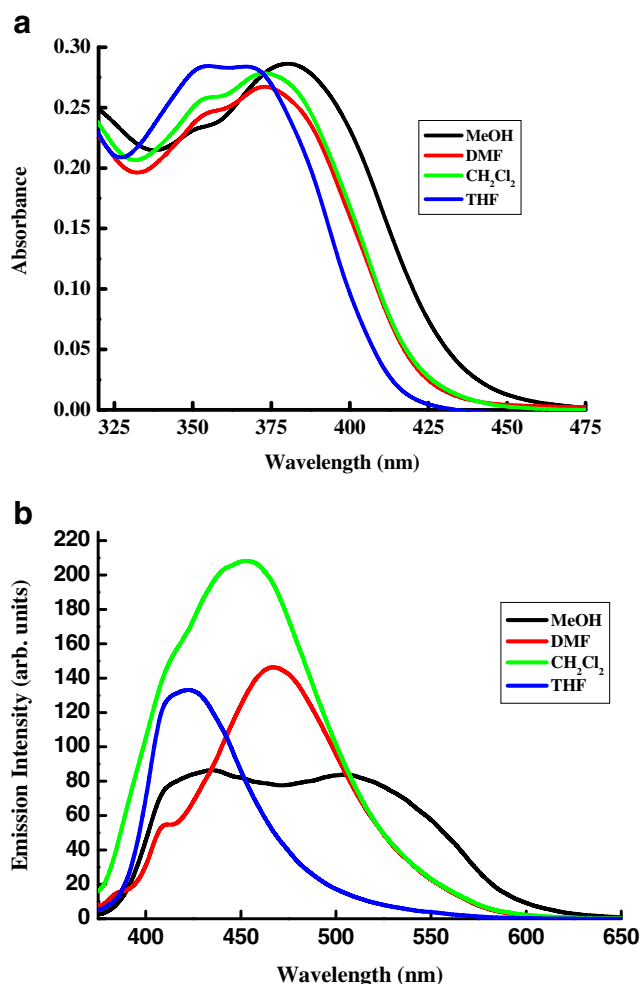

Fig. 3 a Electronic absorption spectra of 1×10^{-5} mol dm^{-3} of chromophore **1** in different solvents. **b** Emission spectra of 1×10^{-5} mol dm^{-3} of chromophore **1** in different solvents
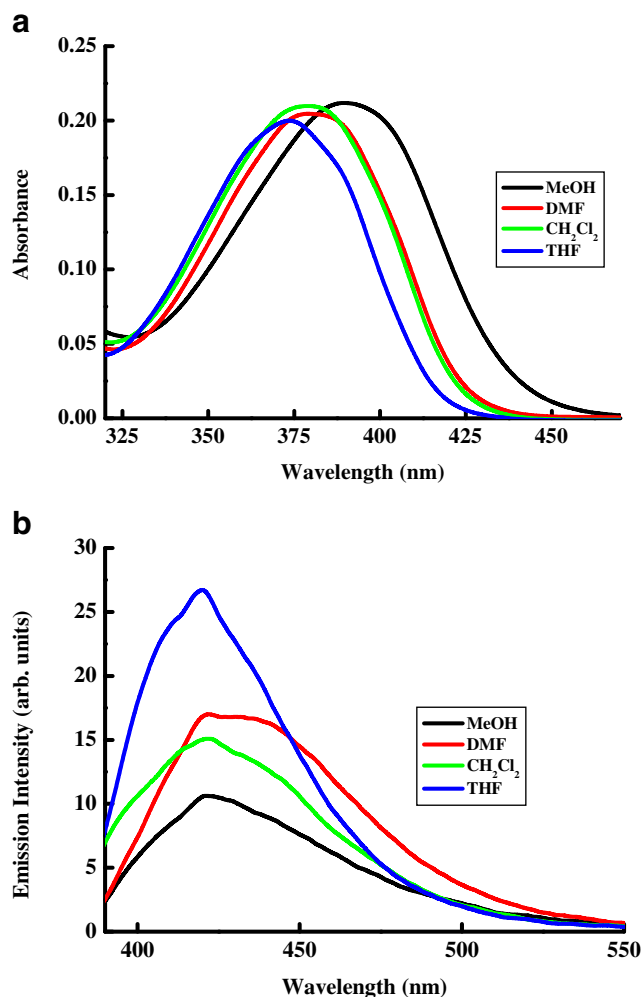
a

b

Fig. 4 **a** Electronic absorption spectra of 1×10^{-5} mol dm^{-3} of chromophore **2** in different solvents. **b** Emission spectra of 1×10^{-5} mol dm^{-3} of chromophore **2** in different solvents

difference can be obtained using the simplified Lippert-Mataga equation as follows [24, 25]:

$$\Delta \overline{v}_{st} = \frac{2 \left(\mu_e - \mu_g \right)^2}{hca^3} \Delta f + \text{Const.} \tag{1}$$

$$\Delta f = \frac{D-1}{2D+1} - \frac{n^2-1}{2n^2+1} \tag{2}$$

where $\Delta \overline{v}_{st}$ is the Stokes–shift [26], which increases with increasing the solvent polarity pointing to stronger stabilization of the excited state in polar solvents, h denotes Planck's constant, c refers to the speed of light in vacuum and a is the Onsager cavity radius. Parameters D and n, in Eq. 2, correspond to the dielectric constant and refractive index of the solvent, respectively. The Onsager cavity radius was chosen to be 4.2 Å because this value is comparable to the radius of a typical aromatic fluorophore [27]. Stokes shifts ($\Delta \overline{v}_{ss}$) of chromophores (**1** & **2**) in different solvents were calculated, as shown in Tables 4 and 5, using the following the equation [24]:

$$\Delta \overline{v}_{ss} = \overline{v}_{ab} - \overline{v}_{em} \tag{3}$$

where $\overline{v}_{ab}$ and $\overline{v}_{em}$ denote the wavenumbers of absorption and emission maxima (cm^{-1}), respectively. The changes in dipole moment ($\Delta\mu$) between the excited singlet and ground state were calculated as 4.08 and −7.37 debye for chromophore 1 and 2 respectively. Positive value of chromophore 1 indicates that the singlet exaited is more polar than the ground state and negative value for chromophore 2 indicating that the ground sate is more polor than the excited state.

The effective number of electrons transition from the ground to excited state is usually described by the oscillator strength, which provides the absorption area in the electronic spectrum. The oscillator strength, f can be calculated using the following equation [28]:

$$f = 4.32 \times 10^{-9} \int \varepsilon(\overline{v}) d\overline{v} \tag{4}$$

where ε is the extinction coefficient (Lmol^{-1} cm^{-1}), and $\overline{v}$ represents the numerical value of wavenumber (cm^{-1}). Oscillator strength values of chromophores (**1** & **2**) in different solvents are reported in Tables 4 and 5. In addition, the transition dipole moment (μ) for chromophores (**1** & **2**) from ground to excited state in Debye was estimated in different solvents using the following relation [29]:

$$\mu^2 = \frac{f}{4.72 \times 10^{-7} \times E_{max}} \tag{5}$$

where E$_{max}$ is the maximum energy of absorption in cm^{-1}.

Table 4 Spectral data of chromophore **1** in different solvents

Solvent	Δf	E_T^N	E$_T$ (30)dyeKcal mol^{-1}	λ_{ab}(nm)	λ_{em}(nm)	ε (M^{-1}cm^1)	f	μ_{12} Debye	$\Delta \overline{v}_{ss}$ (cm$_{-1}$)	Φ_f
MeOH	0.308	1.34	74.26	385	510	28,700	0.73	7.71	6367	0.067
DMF	0.263	1.38	75.63	378	476	26,000	0.56	6.99	5447	0.12
CH$_2$Cl$_2$	0.255	1.39	76.03	376	463	27,900	0.55	6.61	4997	0.15
THF	0.208	1.46	78.11	366	431	28,250	0.46	5.97	4121	0.10

Table 5 Spectral data of chromophore **2** in different solvents

Solvent	Δf	E_T^N	E_T (30)dyeKcal mol^{-1}	λ_{ab}(nm)	λ_{em}(nm)	ε (M^{-1}cm^1)	f	μ_{12} Debye	Δv_{ss} (cm$_{-1}$)	Φ_f
MeOH	0.308	1.34	73.12	391	425	21,270	0.15	3.79	2046	0.003
DMF	0.263	1.35	74.65	383	420	22,030	0.18	3.88	2300	0.005
CH$_2$Cl$_2$	0.255	1.38	75.63	378	418	20,000	0.20	4.02	2532	0.004
THF	0.208	1.41	76.65	373	416	19,800	0.21	41.6	2771	0.008

Fluorescence Polarity Study of Chromophore (1 & 2)

The emission spectra of the two chromophores were measured in different solvents and shown in Figs. 3b and 4b. Their spectral data are also collected in Tables 4 and 5. The emission spectra of these two chromophore consist of one broad band in all the solvent. This band can be assigned to S$_1$-S$_0$ electronic transition. Both chromophore gives the same behavior i.e. chromophores show red shift with increasing solvent polarity (THF to DMF). Chromophore **1** shifted 79 nm chromophore **2** shifted 9 nm on going from THF to DMF indicating the involvement of photoinduced intramolecular charge transfer (ICT) in the singlet excited state than in ground state. Chromophore 2 litle shifted as comparison to dye one because no more π conjugation between donor and acceptor group. Chromophore **1** show the largest red shifted in MeOH because ability of MeOH to form hydrogen bonding with the Chromophore 1 affected the nature (n-π* vs π − π*) of the lowest singlet state. Chromophore **1** often has low lying closely spaced π − π* and n − π* state. Inversion of these two state observed when the polarity and the hydrogen bonding power of solvent increase, because the n − π* state shifted to high energy whereas π − π*) state shifted to lower energy. The solvent dependence of fluorescence spectra has some time called solvatoflurchromism. The empirical Dimroth polarity parameter, E$_T$ (30) and E_T^N of the chromophores 1 & 2 was also calculated according to the following equation [30].

$$E_T^N = \frac{E_T(solvent) - 30.7}{32.4} \tag{6}$$

$$E_T(solvent) = \frac{28591}{\lambda_{max}} \tag{7}$$

where λ_{max} corresponds to the peak wavelength (nm) in the red region of the intramolecular charge transfer absorption of all compounds. The red (bathochromic) shift from THF to indicates that photoinduced intramolecular charge transfer (ICT) occurs in the singlet excited state, and the polarity of compounds, therefore, increases on excitation.

The fluorescence quantum yield (φ_f) was measured using the optically diluted solution to avoid reabsorption effect (absorbance at excition wave relative method with solution of Fluorescein in MeOH as reference standard [31, 32]. The

following relation has applied to calculate the fluorescence quantum yield:

$$\phi_f(s) = \varphi_f(r) \frac{F_{(s)}\{1 - \exp(-A_{ref}\ln10)\} \times n^2s}{F_{(ref)}\{1 - \exp(-A_s\ln10)\} \times n^2r} \tag{8}$$

where F denotes the integral of the corrected fluorescence spectrum, A is the absorbance at the excitation wavelength, and n is the refractive index of the medium. The subscripts "s" and "r" refer to sample and reference, respectively. Flurescence quantum yield of chromophores 1 & 2 in different solvent are also listed Tables 4 and 5.

Frontier Orbitals Analysis

The frontier orbitals; highest occupied molecular orbital (HOMO) and lowest unoccupied molecular orbital (LUMO) of chemical species are very important in defining their stability and reactivity [33]. The molecules having higher energy HOMOs have a tendency to donate electrons to the molecules with low energy LUMOs i.e. having empty molecular orbitals. The total energy, HOMO, LUMO, hardness (η), ionization energy (IE), electron affinity (EA), electrostatic potential map, of chromophore **1** and **2**, were calculated. The obtained computational results showed that the frontier molecular orbital energy gap (ΔE_{gap} = 3.91 eV) of chromophore **1** is lower than chromophore **2** (ΔE_{gap}: 4.30 eV) (Fig. 5). The hardness (η) index corresponds to the energy gap (ΔE_{gap}) between HOMO and LUMO and is used to predict the molecular reactivity. Larger the ΔE_{gap}, harder is the molecule, and less reactive it is. Since according to Pearson [34] soft molecules are more reactive than hard molecules. The hardness is also associated with the stability of the chemical system. The hardness and stability are directly proportional to each other. Accordingly, it is concluded that chromophore **1** is comparatively more reactive and less stable than chromophore **2**.

The ionization energy (IE) can be expressed through HOMO orbital energies as IE = − ε_{HOMO} and electron affinity (EA) can be expressed through LUMO orbital energies as EA = − ε_{LUMO} [35]. Accordingly, the IE of chromophore **1** is 5.30 eV and of chromophore **2** is 5.45 eV. The EA of chromophore **1** is 1.39 and of chromophore **2** is 1.15 eV. This indicates that IE of chromophore **2** is higher than
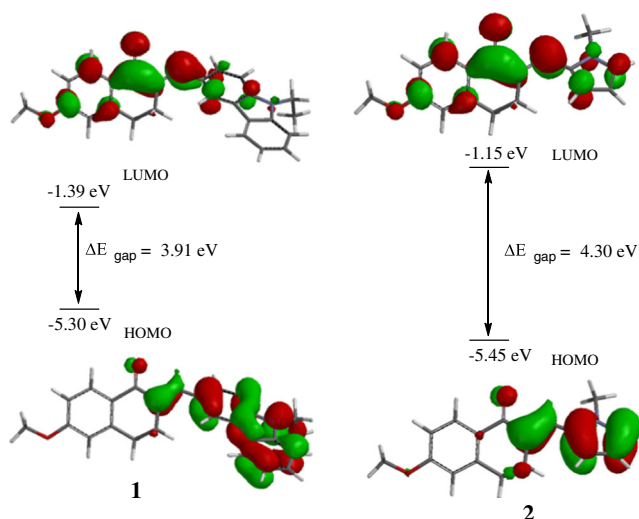
Fig. 5 Energy gap between HOMO and LUMO orbitals of chromophore 1 and 2

chromophore **1** while EA of chromophore **2** is lower than chromophore **1**. The electrostatic potential map illustrates the reactive sites of the molecules (Fig. 6). The electrostatic potential energy map of both the molecules showed that the large electrostatic potential surfaces are located at oxygen atoms. Hence, it is concluded that the most reactive site are due to the presence of oxygen atoms i.e. high electron density atoms. Total energy of chromophore **1** calculated is −1209.93714 au and of chromophore **2** is −863.224564 au. Total energy of chromophore **1** is higher than chromophore, this is quite obvious as chromophore **1** has higher molecular weight than chromophore **2**. It is concluded that physicochemical properties and frontier orbital has been demonstrated
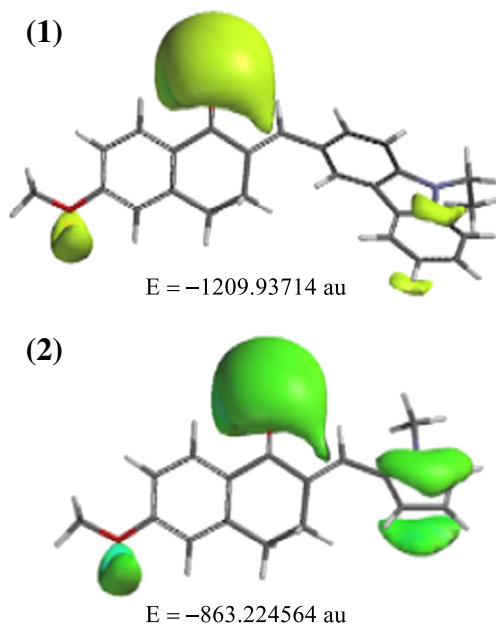

Fig. 6 Electrostatic potential map of chromophore 1 and 2. The total energies calculated with RB3LYP method are also given

using ab initio molecular orbital theory. These results represent a good approximation of the stability and reactivity of the molecules.

Conclusion

Two push-pull chromophores were synthesized by the reaction appropriate aldehyde and 6-methoxy-1,2,3,4-tetrahydronaphthalin-1-one under microwave irradiation by Knoevenagel condensation. Structure of the chromophores was confirmed by single crystal X-ray. Physicochemical studies of the chromophore including singlet absorption, extinction coefficient, Stokes shift, oscillator strength and dipole moment were investigated on the basis of the polarity of solvent. The absorption spectra of chromophore **1** and **2** exhibit an intramolecular charge transfer band; which showed a positive solavotochromism in different solvents. The emission spectra of the dyes also reveal the intramolecular charge transfer band character. These findings confirm that there is a significant electron transfer between the donating moiety and the accepting fragment through the π conjugated. Indeed, the physicochemical properties; the total energy, HOMO, LUMO, hardness (η), ionization energy (IE), electron affinity (EA), electrostatic potential were also calculated using density functional theory. It is concluded that chromophore **1** is comparatively softer and reactive than chromophore **2**.

References

1. Khan SA, Asiri AM, Kumar S, Sharma K (2014) Green synthesis, antibacterial activity and computational study of pyrazoline and pyrimidine derivatives from 3-(3,4-dimethoxy-phenyl-1-(2,5-dimethyl-thiophen-3-yl)-propenone. Eur J Chem 4:459–464

2. Asiri AM, Khan SA (2012) Synthesis, characterization, and in vitro antibacterial activities of macromolecules derived from bis-chalcon. J Heterocycl Chem 49:1434–1438

3. Wang Y, Yang Z, Chen Z (2008) Synthesis, characterization and DMA-binding properties of four Zn(II) complexes with bis(pyrrol-2-yl-methyleneamine) ligands. Bioorg Med Chem 18:298–303

4. Marwani HM, Asiri AM, Khan SA (2013) Spectral, stoichiometric ratio, physicochemical, polarity and photostability studies of newly synthesized chalcone dye in organized media. J Lumin 136:296–302

5. Asiri AM, Khan SA, Al-Amodi MS, Alamry KA (2012) Synthesis, characterization, absorbance, fluorescence and non linear optical properties of some donor acceptor chromophores. Bull Kor Chem Soc 33:1900–1906

6. Asiri AM, Khan SA, El-Hallag SI (2011) Electrochemical studies of some carbazole derivatives via cyclic voltammetry and convolution - deconvolution transforms. J New Mater Electrochem Syst 4: 251–258

7. Carlini C, Ciardelli F, Donati D, Gurzoni F (1983) Polymers containing side-chain benzophenone chromophores: a new class of highly efficient polymerization photoinitiators. Polymer 24:599–606

8. Asiri AM, El-Daly SA, Khan SA (2012) Spectral characteristics of 4-(p-N,N-dimethyl-aminophenylmethylene)-2-phenyl-5-oxazolone (DPO) in different media. Spectrochim Acta, Part A 95:679–684

9. He M, Zhou Y, Liu R, Dai J, Cui Y, Zhang T (2009) Novel nonlinearity-transparency−thermal stability trade-off of thiazolylazopyrimidine chromophores for nonlinear optical application. Dyes Pigments 80:6–10

10. Asiri AM, Khan SA (2011) Synthesis, characterization and optical properties of mono- and bis-chalcone mater. Letters 65:1749–1752

11. Asiri AM, Khan SA, Marwani HM, Sharma K (2013) Synthesis, spectroscopic and physicochemical investigation of environmentally benign heterocyclic Schiff base derivatives as antibacterial agents on the bases of in vitro and density functional theory. J Photochem Photobiol B 120:82–89

12. Asiri AM, Marwani HM, Khan SA (2014) Spectroscopic investigation of novel donor–acceptor chromophores as specific application agents for opto-electronics and photonics". J Saudi Chem Soci 18:392–397

13. Watson BT, Christiansen GE (1998) Solid phase synthesis of substituted quinolin-2(1H)-one-3-carboxylic acids via an intramolecular knoevenagel condensation. Tetrahedron Lett 39:6087–6090

14. Liu Q, Ai H, Li Z (2011) Potassium sorbate as an efficient and green catalyst for knoevenagel condensation. Ultrason Sonochem 18: 477–479

15. He M, Twieg R, Gubler U, Wright D, Morner WE (2003) Synthesis and properties of glassy organic multifunctional photorefractive materials. Opt Mater 21:353–357

16. Biradar JS, Sasidhar BS (2011) Solvent-free, microwave assisted Knoevenagel condensation of novel 2,5-disubstituted indole analogues and their biological evaluation. Eur J Med Chem 46:6112–6118

17. Agilent CrysAlis PRO (2012) Agilent technologies, Yarnton, England

18. Sheldrick GM (2008) A short history of SHELX. Acta Crystallogr A64:112–122

19. Barbour LJ, Seed X (2001) A software tool for supramolecular crystallography. J Supramol Chem 1:189–193

20. Bernstein J, Davis RE, Shimoni L, Chang NL (1995) Patterns in hydrogen bonding functionality and graph set analysis in crystals. Angew Chem Int Ed Engl 34:1555–1573

21. Spartan'08 Version 1.2.0, Wavefunction, Inc., 18401 Von Karman Ave., Suite 370, Irvine, CA 92612, USA

22. Asiri AM, Khan SA, Marwani HM, Sharma K (2013) Synthesis, spectroscopic and physicochemical investigations of environmentally benign heterocyclic Schiff base derivatives as antibacterial agents on the bases of in vitro and density functional theory. J Photochem Photobiol B: 120:82–89

23. Khan SA, Asiri AM, Al-Thaqafy SH, Faidallah HM, El-Daly SA (2014) Synthesis, characterization and spectroscopic behavior of novel 2-oxo-1,4-disubstituted-1,2,5,6-tetrahydrobenzo[h]quinoline-3-carbonitrile dyes. Spectrochim Acta A 133:141–149

24. Dey JK, Dogra SK (1991) Solvatochromism and prototropism in 2-(aminophenyl) benzothiazoles. Bull Chem Soc Jpn 64:3142–3152

25. Acree WE, Wilkins DC, Tucker SA, Griffin JM, Powell JR (1994) Spectrochemical investigations of preferential solvation. 2. Compatibility of thermodynamic models versus spectrofluorometric probe methods for tautomeric solutes dissolved in binary mixtures. J Phys Chem 98:2537–2544

26. Kumar S, Rao VC, Rastogi RC (2001) Excited-state dipole moments of some hydroxycoumarindyes using an efficient solvatochromic method based on the solvent polarity parameter, E_T^N. Spectrochim Acta A 57:41–47

27. Ravi M, Samanta A, Radhakrishnan TP (1994) Excited state dipole moments from an efficient analysis of solvatochromic stokes shift data. J Phys Chem 98:9133–9136

28. Ravi M, Soujanya T, Samanta A, Radhakrishnan TP (1995) Excited-state dipole moments of some coumarin dyes from a solvatochromic method using the solvent polarity parameter, E_T^N. J Chem Soc Faraday Trans 91:2739–2742

29. Turro NJ (1995) Molecular photochemistry (frontiers in chemistry), 1st edn. W. A. Benjamin, Inc., Reading, p. 286

30. Coe BJ, Harris JA, Asselberghs I, Clays K, Olbrechts G, Persoons A, Hupp JT, Johnson RC, Coles SJ, Hursthouse MB, Nakatani K (2002) Quadratic nonlinear optical properties of N-aryl stilbazolium dyes. Adv Funct Mater 12:110–116

31. El-Daly SA, Asiri AM, Khan SA, Alamry KA (2013) Spectral properties and micellization of 1-(2,5-Dimethyl-thiophen-3-yl)-3-(2,4,5-trimethoxy-phenyl)-propenone (DTTP) in different media. J Lumin 134:819–824

32. El-Daly SA, Asiri AM, Alamry KA, Khan SA (2013) Spectroscopic studies and laser activity of 3-(4-dimethylamino-phenyl)-1-(2,5-dimethyl-furan-3-yl)-propenone (DDFP): a new green laser dye. J Lumin 137:6–14

33. Fukui K, Yonezaw T, Shingu H (1952) A molecular orbital theory of reactivity in aromatic 29 hydrocarbons. J Chem Phys 20:722–725

34. Pearson RG (1987) Recent advances in the concept of hard and soft acids and bases. J Chem Educ 64:561–567

35. Zhan CG, Nichols JA, Dixon DA (2003) Ionization potential, electron affinity, electronegativity, hardness, and electron excitation energy: molecular properties from density functional theory orbital energie. J Phys Chem A 107:4184–4195